

Fracture strength of individual titanium matrix coated monofilament silicon carbide fibre

J. Laffargue, J. Liu, P. Bowen

The effects of gauge length on fracture tensile strength of individual titanium matrix coated silicon carbide fibres have been investigated. Weibull statistics were used to represent the variability of the fracture strength of the Amercom Trimarc silicon carbide fibres. It shows a significant variation in strength over 1, 20 and 100 mm etched gauge length. The Ti-6Al-4V matrix is removed by electropolishing. A linear location technique has been performed with two acoustic sensors. Failure occurred within the gauge length and events of 98 dB with high energy released are characteristic of fibre failure. Using fractography, low strength fibres were found to fail from surface flaws, while core fracture initiation is typical of high strength fibres. A proposed bimodal Weibull cumulative failure probability function is well suited to characterise the two distinct fracture mechanisms within the fibre populations for 1 and 20mm etched gauge lengths. Fatigue testing shows that the strength of monofilaments can be degraded by cycling loading and mechanism can be identified fractographically. Matrix defects due to processing initiate fatigue cracks. Debonding occurs between the carbon coating layer and the silicon carbide fibre in the monofilament during tension-tension fatigue tests.

Parole chiave: materiali compositi, frattura, prove meccaniche

INTRODUCTION

The development and application of titanium metal matrix composites (TiMMC) for increase in engine thrust to weight ratio and the reduction in mission fuel burn, require a thorough understanding of strength characteristics of the reinforcing fibre because many of the properties that make TiMMCs attractive for use in gas turbine engine components are controlled by fibre strength.

The matrix coated fibre process is a relatively new fabrication route for TiMMCs, which uses high rate physical vapour deposition (PVD) to pre-coat continuous fibre with a thick layer of matrix alloy. The coated fibres are then laid-up and hot pressed into the finished TiMMC. The process is well suited to the filament winding of product as rings, blades, discs and tubes (1-3).

However the properties on fibre strength in the intermediate stage of monofilament fibre coating is still not clear. Consolidation and use of TiMMCs temperatures does not significantly reduce the fibre strength when fibres fail from internal initiations, but a bimodal distribution in strength is developed when surface flaws were created after heat treatment during fabrication process (4).

The mechanisms of fibre strength degradation are often attributed to surface flaws and internal core interface flaws (5), these observations are typical for W-core SiC fibres. Also during the CVD process, a chemical reaction between the tungsten core and the deposited SiC occurs to form a reaction layer of WC at the interface (6), this can also be a reason for fibre strength degradation.

Using Weibull statistics, the fracture of ceramics is well

established (7,8). Such methods can be used to describe fibre strength and they can also be used to predict the tensile strength distribution of single composites and bundle of composite fibres if we assume that composite failure is caused by fibre fracture.

The smallest gauge length simulates the approximate debonded length of a bridged matrix crack in fatigue crack growth studies on fully consolidated TiMMCs and the larger gauge length provides accurate comparisons for the prediction of composite strength.

EXPERIMENTAL

Materials

Continuous SiC filaments are processed in a tubular glass reactor using chemical vapour deposition (CVD). The reinforced fibre examined in this study was a SiC fibre manufactured by Amercom, Inc., designated as Trimarc, with a diameter of 129 μm . It has a tungsten core of 11 μm and an outer carbon coating that protects the fibre during the matrix consolidation and promote interface debonding in use.

The Trimarc fibres were matrix coated by 3M in the USA and a PVD process at a temperature of 500°C during 8 hours was used. Ti-6Al-4V (atomic percent) of 45 μm thickness was deposited to give an overall diameter of matrix-coated fibre of 220 μm . So the volume fraction of fibre in the monofilament composite was 35% (fig.1).

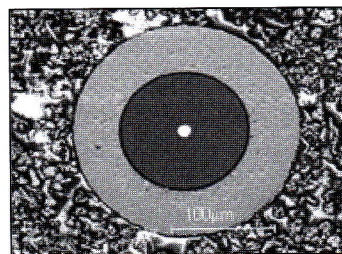


Fig.1: secondary electron micrograph of as received MCF Trimarc.

Fig.1: micrografia con elettroni secondari di un MCF Trimarc come ricevuto.

J. Laffargue, J. Liu, P. Bowen

Interdisciplinary Research Centre (IRC) in Materials for High Performance Applications/
School of Metallurgy and Materials, The University of Birmingham, UK

Paper presented at the 7th European Conference EUROMAT 2001,
Rimini, 10-14 June 2001 organised by AIM

Procedure

The Titanium alloy matrix Ti-6Al-4V was removed along 1, 20 and 100 mm from the as-received (AR) monofilament composite by electro polishing. The electrolyte solution was 6 percent perchloric acid (HClO_4) saturated with 34 percent butan-1-ol ($\text{CH}_3(\text{CH}_2)_3\text{OH}$) and 60 percent methanol (CH_3OH). The power supply delivered a continuous current of approximately 0.4 A/cm^2 through a thick nickel cathode plate, the fibres were acting as the anode. Five monofilaments were electro polished simultaneously leaving intact the SiC fibres with the outer carbon layer (fig.2). Particular

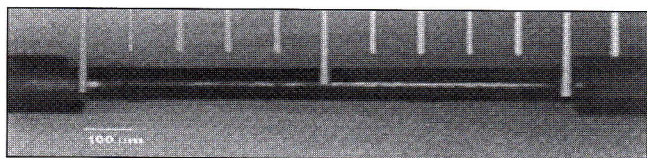


Fig.2: Typical 1mm etched gauge length.

Fig.2: Tipica lunghezza di riferimento di 1mm

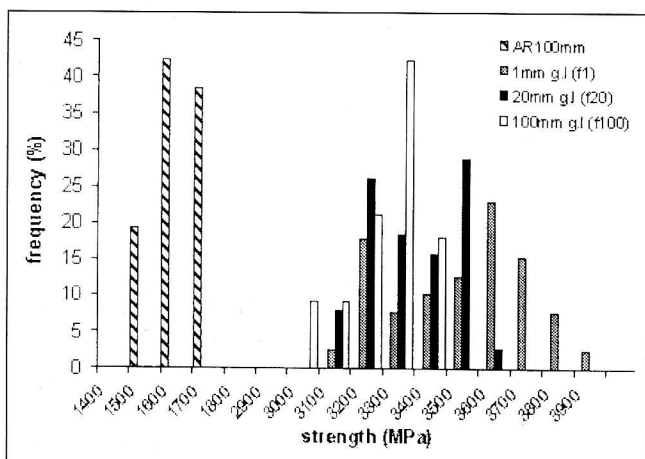


Fig.3: strength distributions of as received MCF, and etched gauge length of 1mm, 20mm and 100mm.

Fig.3: distribuzione della resistenza di un MCF come ricevuto e lunghezza di riferimento di 1mm, 20mm e 100mm

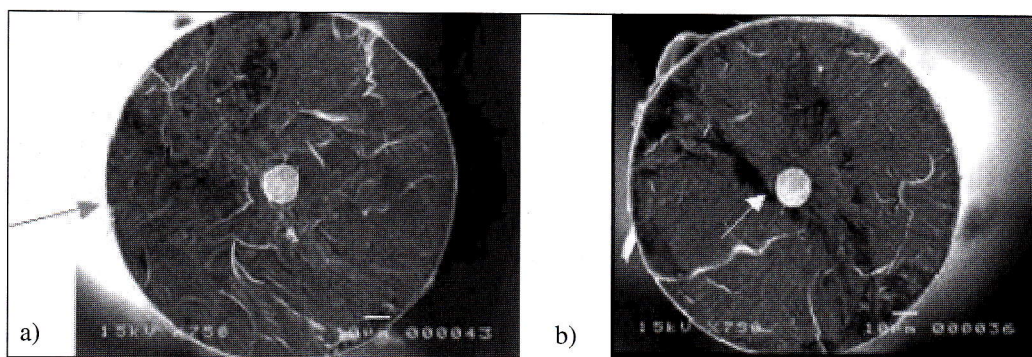


Fig.4: Fractography of 20 mm etched gauge length fibres under tensile test; a) $\sigma=3057 \text{ MPa}$ and b) $\sigma=3533 \text{ MPa}$. Failure initiation sites are arrowed.

Fig.4: Frattografia di fibra con lunghezza di riferimento di 20 mm, sottoposta a prova di tensione; a) $\sigma=3057 \text{ MPa}$ e b) $\sigma=3533$. Le zone in cui ha inizio la rottura sono contrassegnate da una freccia.

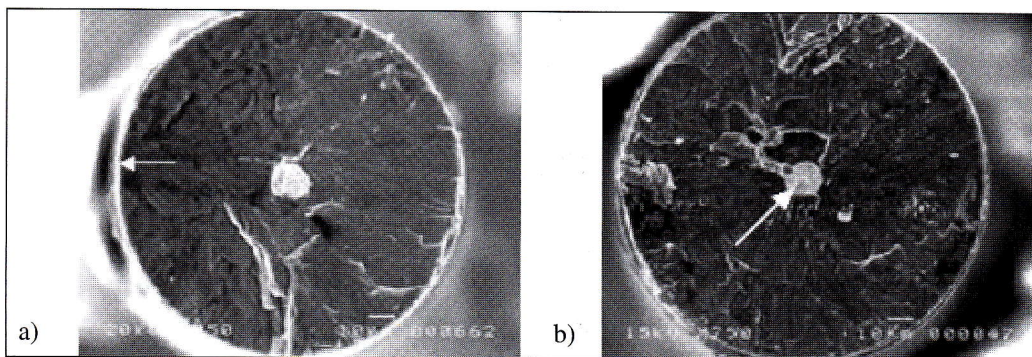


Fig.5: Fractography of 1 mm etched gauge length fibres under tensile test; a) $\sigma=3020 \text{ MPa}$ and b) $\sigma=3798 \text{ MPa}$. Failure initiation sites are arrowed.

Fig.5: Frattografia di fibra con lunghezza di riferimento di 1 mm, sottoposta a prova di tensione; a) $\sigma=3020 \text{ MPa}$ e b) $\sigma=3798$. Le zone in cui ha inizio la rottura sono contrassegnate da una freccia.

attention was taken in handling the fibre to not affect the fibre strength measured during subsequent tensile testing. The fibres were finally cleaned with acetone to remove any residual etchant.

Forty etched fibres in each condition were tensile tested. The single fibre tensile tests were conducted on an ESH servo-hydraulic testing system of 250 kN capacity, but equipped with a 1kN load cell calibrated independently to a full-scale load range of 100 N. All test were conducted at room temperature under a piston ramp rate of 0.1 mm/min . To avoid stress concentration around the gripping zone the grip gauge length was maintained constant and slightly greater than the etched gauge length. So the result of 39 fibres of 1 mm etched gauge length, 39 fibres of 20 mm etched gauge length, 33 fibres of 100 mm etched gauge length and 35 fibres of 100 mm matrix coated gauge length were analysed statistically using Weibull distributions.

Tension-tension fatigue tests were performed at room temperature on as-received monofilament composite with the same ESH servo-hydraulic testing system of 250 kN capacity. These specimens were cycled at a frequency of 1 Hz, with a sinusoidal waveform at a stress ratio $R (\sigma_{\min}/\sigma_{\max})$, of 0.1. Most of specimens tested failed within the gauge length of 100 mm.

The precise location of fibre failure during tensile and fatigue tests was determined by acoustic emission. Two resonant piezoelectric AE sensors PICO 3276 of maximum sensitivity 500 kHz were glued on the width-surface of the grips. The AE signals from each sensor were amplified by a pre-amplifier with a gain of 40 dB, and then processed by a fully digital two channels MISTRAS 2001 system. The AE threshold was set to 45 dB. According to the calibration method described in (9), the speed of the longitudinal AE wave in the monofilament was found to be $\approx 7000 \text{ m.s}^{-1}$, using fibres with a known failure location within the 1mm etched gauge length.

When fractures surfaces could be preserved, they were collected and mounted for examination by scanning electron microscopy to determine the initial site for tensile failure.

The fractography of single fibres was examined by using a JSM 5410 scanning electron microscopy under an accelerating voltage set at 20 kV. The "matching" pair of fracture

surfaces of more than 20 fibres were examined with the SEM. The greatest attention was taken to match the two fracture surfaces.

RESULTS

All the etched fibres failed within a strength range of 2968 to 3848 MPa, and within 1525 to 1794 MPa for as-received matrix-coated fibres. The mean strength of the as-received composite is 1672MPa. The strength distribution of the three groups of etched gauge length fibres (1mm (f1), 20mm (f20) and 100mm (f100)), and of the as-received monofilament (AR100mm) are shown in the figure 3. Obviously distributions of 1mm and 20mm etched gauge length do not show a normal distribution like the distribution of 100mm etched gauge length, which have a mean strength of 3199 MPa. A bimodal distribution should be more appropriate for distributions f1 and f20, i.e. two different fracture mechanisms, considering that they exhibit two main peaks of strength frequency at 3552 and 3159MPa, 3447 and 3154MPa, respectively.

According to the experimental values σ , $\Delta\sigma$, $\Delta\sigma/\sigma$, each population is well normally distributed for these brittle samples. The average fibre strength value of all tensile results increases from 3199, 3289 to 3458 MPa when the etched gauge length is reduced (respectively f100, f20 and f1). Errors in strength variation lie between 3 and 6 % with a small change in the standard deviations (73, 106, 139 and 214 MPa for AR100, f100, f20 and f1 respectively). These small changes characterize a uniform partition of flaws along the fibre and the increase in $\Delta\sigma$ value as the gauge length is reduced denotes the difficulty of controlling the fibre strength for a small etched length. The significance in the variation in mean strength between the three groups of etched fibres was conducted using a statistical t-test for a given level of confidence. It results that the increase in mean fibre strength is significant at 95% of level of confidence regarding normal strength distributions.

Fractography of tested fibres was used to distinguish between the high and low strength fibres.

Two types of fibre fractures were observed, those that were initiated from the tungsten core and those that initiated from surface flaws.

Fracture surface of etched fibres over 100 mm gauge length were very hard to collect hence the lack of matched surfaces does not give an accurate analysis of the whole population, therefore most fractures initiated from surface flaws. In the population of 20 mm etched gauge length fibres, two distinct initiation sites can be noticed. For fibres with strength lower than 3300 MPa, fractures start from surface defects, as seen in the typical fracture surfaces in figure 4a, the "hackle zones" start from the surface of the fibre, and larger size of flaws are found on fibres with very low strength. Fibres with strength higher than 3300 MPa have typical core initiated fracture, where "hackle zones" started from the tungsten core (fig.4b) and the ridges are finer.

In the population of 1 mm etched gauge length fibres, it appears that there are also two types of fracture initiations of the same nature as seen in 20 mm gauge length fibres. Fibres

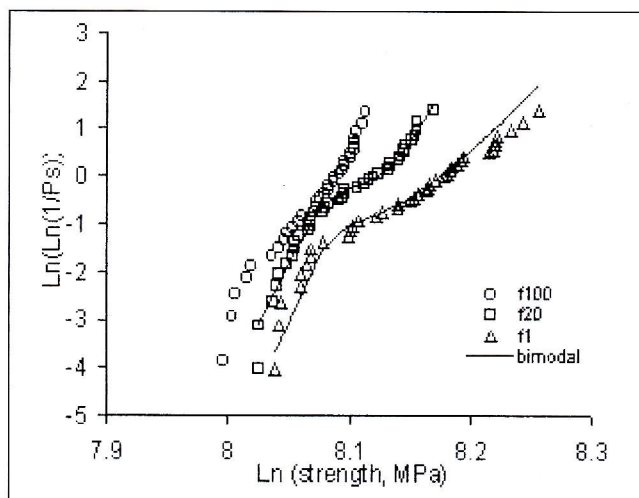


Fig.6: Weibull distributions of 1mm (f1), 20mm (f20), 100mm (f100) etched gauge length fibres.

Fig.6: Distribuzioni di Weibull per fibre con lunghezze di riferimento di 1mm (f1), di 20mm (f20), di 100mm (f100).

with higher strength than 3300 MPa have radiating lines from the centre (fig.5a) and the tungsten core seems to be the initiation site of failure, while fibres with lower strength than 3300 MPa exhibit surface flaws (fig.5b).

Fracture surface morphologies of low strength fibre have characteristic feature of large smooth fracture surfaces and internal failures from high strength fibres initiated at the WC reaction layer.

A typical observation of 1mm and 20 mm gauge length fibres is that, fibres with strength around 3300 MPa have a morphology composed of larger ridges with "hackle zones" from the core and some radiating lines on the surface. However, no obvious predominant initiation sites can be distinguish which perhaps indicated that both fracture mechanics may be balanced between the two type of flaws in this result in a medium fracture strength.

A Weibull statistical analysis of the tensile strength distribution for etched matrix coated fibre over 1, 20, and 100 mm gauge length and as-received monofilament was performed. Figure 6 shows the Weibull distributions of the three groups of etched fibres. It is obvious that a uni-modal distribution is insufficient to describe all the populations. As the gauge length is decreased, a more distinct bi-modal distribution is shown and the strength value of $\sigma_c = 3270$ MPa ($\ln\sigma_c = 8.09$) appears to be critical. Although f100 follows a almost straight line ($m=35$ and $\sigma_0 = 3247$), Weibull plot shows for population f1 and f20 two linear regions on both sides of the critical value $\ln\sigma_c = 8.09$ MPa. So if the fibres in each of the two strength regions are regarded as two sub populations and the data are processed separately, the data fall into a straight line.

This means that sub populations f1 and f20 follow uni modal Weibull distribution. The results of the Weibull parameters m and σ_0 are listed in table 1. Also, the shape parameter m considered in each strength region is high, which means that the fibre defects were well controlled (from processing

Table.1: Weibull parameters of bi-modal distributions

Tab.1: Parametri Weibull di distribuzioni bi-modali

	Gauge length	p% of fibres	Low strength ($s < 3270$ MPa)		High strength ($s > 3270$ MPa)	
			m_1	σ_{01} (MPa)	m_2	σ_{02} (MPa)
Etched matrix	1 mm (f1)	23 (9/39)	77	3222	77 (30/39)	3587
	20 mm (f20)	47 (19/40)	59	3413	53 (21/40)	3754

and manipulation) and that each distribution has a uniform flaw partition along the fibre.

Fibre strength is dominated by the presence of the type of flaws within the fibre length. Fibres whose the fracture has initiated from surface flaws have low strength ($\sigma < 3270$ MPa). They are comprised in a narrow strength range because surface flaws affect the fibre strength catastrophically. However high strength fibres ($\sigma > 3270$ MPa) have generally internal flaw fracture initiation and it appear that the interfacial W/SiC flaw does not reduce the fibre tensile strength considerably. Hence the number of high strength fibres is larger for a smaller gauge length. For a long fibre gauge length (100mm) the chance of finding surface flaws is much bigger so it can be considered that it will have always a defect within this length that will limit the fibre strength as the fibre failed at its weakest point, i.e. surface defects. Thus it follows a uni-modal distribution.

So in high strength fibres, the gauge length controls the increase in mean strength as the distributions move away significantly from each other and for low strength fibres, surface flaws maintain low strength avoiding significant variation in strength.

For each strength region, fracture mechanisms are different and correspond well to these described by SEM fractography within a given strength range.

Fibre failure locations were determined by acoustic emission. All the fibres failed within the considered gauge length. It is shown that the amplitude and the energy of the AE event recorded by the sensors are characteristic of fibre failure, 98 dB in amplitude with a high energy released around 20000 depending of the sensitivity of each sensors. Although it might have an attenuated energy due to the sensors glued on the grips and not directly on the specimen, the energy is still high compared to the events recorded before final failure in a tensile test.

Matrix-coated fibres of 100 mm gauge length were fatigued to produce a total life S-N curve. Results are shown in figure 7, and the repeatability of number of cycles to failure was acceptable.

An effect of fatigue loading is noticed and the number of cycles to failure drops as the load is increased. Usually brittle materials are considered not to exhibit fatigue behaviour moreover the fibre is supposed to maintain the strength of the monofilament composite.

From SEM observations, fractures morphologies of fibres were affected by tension-tension fatigue loading. It appears that fibres whose have been fatigued with a lower stress range have finer surface while when higher applied stress range is applied hackles are found within smooth surface. Thus,

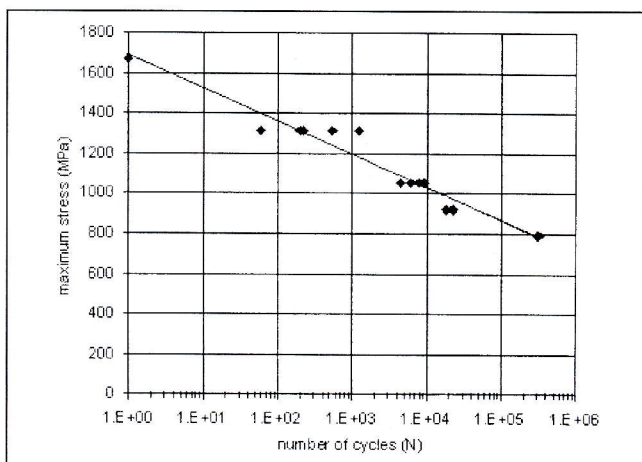


Fig.7: Total fatigue life S-N curve of as received MCF.

Fig.7: Curva S-N di vita a faticatotale per un MCF come ricevuto.

the fibre strength might have been affected by fatigue loading as there is a difference in fibre morphology and they most failed in loading up.

Here in high fatigue loading range (from survival in a given tensile strength range) the fibre is weakened but the ductility of the matrix appears to play an important role in the fatigue of composite. Nevertheless, previous authors (10) show that high strength fibres (SCS-6 Textron) can be significantly affected by fatigue loading.

All fibres have been broken where surface flaws were present. Matrix processing defect act as a natural notch where the fatigue is initiated. The non-consolidate matrix unable us to see striations in the matrix microstructure which is characteristic of fatigue fracture mechanic. Debonding occur between the matrix and the carbon coating and not between carbon coating and fibre.

DISCUSSION

The model proposed describes two distinct fracture mechanisms. Fibre populations of 1mm and 20mm etched gauge length can be described by bi-modal function expressed as eq.1:

$$F(\sigma) = 1 - p \cdot \exp\left\{-L \left(\frac{\sigma}{\sigma_{01}}\right)^{m_1}\right\} - q \cdot \exp\left\{-L \left(\frac{\sigma}{\sigma_{02}}\right)^{m_2}\right\} \quad (\text{Eq.1})$$

Where m_1 , m_2 and σ_{01} , σ_{02} are respectively the Weibull parameters for low strength and high strength. p and q are the percentages of fibre include in these strength ranges (see table 1). Distributions f_1 and f_2 are in good agreement with the experimental results. The validity of eq.1 can be verified in figure 6 by the good correlation between calculated (bi-modal) and experimental data. This equation derives from the model proposed in(9) which seems to be more appropriate than the bi-modal function described in(5) by Goda. Indeed, here we are able to distinct failures from surface and internal flaws.

As it has been reported that the production of surface flaws on extracted fibres from TiMMCs is increased after heat treatment, the fibre strength of 1mm debonded length in bridged fibre model can thus be expressed from bimodal distribution.

The strength of a unidirectionally reinforced composite in the fibre direction may be estimated using the rule of mixtures (ROM). Using the mean strength of 100 mm etched gauge length fibre matrix-coated fibres, the matrix yield strength, σ_m , is evaluated at 857 MPa. With σ_m after consolidation (~960 MPa,(11) the mean coated-fibre strength is 1740 MPa, which is reasonably close to the measured composite tensile strength of 1672 MPa.

Fibres can be assumed to behave as a bundle of fibre: This means that the number of fibres is large, that fibres have identical load-elongation curves and that if a fibre breaks it no longer bears any load. So the fibre bundle strength can simulate the strength of bridging fibre in fully consolidated composite with a gauge length corresponding to the debonded length, and the value of the fibre bundle strength, σ_B , of fibres with bi-modal and uni-modal Weibull distribution can be calculated following(7) the equation expressed as:

$$\sigma_B = \max\{\sigma[1 - F(\sigma)]\} \quad (\text{Eq.1})$$

Here σ is the stress carried by each fibre and $F(\sigma)$ is the cumulative failure probability for uni modal and bi modal (eq.1) distributions.

The σ_B values calculated are 3349 MPa for 1mm, 3388 MPa for 20 mm and 3044 MPa for 100 mm etched gauge length fibres. σ_B values of fibre bundle strengths are lower than the mean fibre strengths apart for 20 mm etched gauge length, but it appears that there is no decrease in fibre bundle strength when the gauge length is increased from 1mm to 20 mm. σ_B values for 1 mm and 20mm etched gauge length are almost identical. Therefore, increasing to 100 mm the etched gauge length fibre decrease significantly the fibre bundle strength by 10% and 11%, respectively from 1mm and 20mm etched gauge length. Thus, values from fibre bundle strengths remain almost constant for a small variation in gauge length.

Modelling studies, i.e shear lag model, suggest that in situ fibre fracture strengths in the wake of a crack bridging fibre is higher than those measured from test piece with much longer gauge lengths. It has been confirmed here that a decrease in gauge length up to 1mm has induced an increase in the mean fibre strength.

SUMMARY

- There is a significant increase in the mean tensile strength fibre when the etched gauge length is reduced. 1 mm and 20 mm etched gauge length fibres demonstrate a bimodal Weibull distribution in strength and eq.1 is a well suited model for bimodal distribution.
- Acoustic Emission characterises fibre failure events at 98 dB with high energy released.

- Two failure initiations can be distinguished, surface flaws and internal WC flaws corresponding to low and high strength fibres, respectively.
- Fatigue loading affects strength of the matrix coated fibre.

REFERENCES

- 1) C. M. Ward-Close, M. R. Winstone and P. G. Partridge, *Materials&Design*, 24(2), (1994), p.67.
- 2) M.J. Wood, C.M Ward-Close, *Mater. Sci. Eng.*, A192-193 (1995), p.590.
- 3) C.M. Ward-close, *Mater. Sci. Eng*, A263 (1993), p.314.
- 4) M.L Gambone, *Acta Metallurgica*, 34(3) (1996), p507.
- 5) M.L Gambone and F.E. Wawner, *Journal of composites materials* 31 (1997), p.1062.
- 6) M.L Gambone and D.B Gundel, *Key Eng. Mater*, 127-131 (1997), p.1251.
- 7) A.Kelly and N.H. MacMillan, *Strong solids*, 3rd edition, Clarendon Press, Oxford (1986).
- 8) A.Khalili, K.Kromp, *Journal of materials science* 26 (1991) 6741-6752.
- 9) J.Lui and P.Bowen, *Spatial location of fibre failure during fatigue of TiMC reinforced by SiC fibres*, University of Birmingham, 2000.
- 10) J.Liu and P.Bowen, *Strength of SCS-6 fibres*, Submitted for publication, 2001.
- 11) J.Liu, *Fatigue Crack Growth Resistance and Transverse Tensile Behaviour of TiMMC*, PhD thesis University of Birmingham, 1997.

ABSTRACT

RESISTENZA ALLA FRATTURA DI FIBRE MONOFILAMENTO DI CARBURO DI SILICIO CON RICOPERTURA A MATRICE DI TITANIO

Sono stati esaminati gli effetti della lunghezza del tratto di riferimento sulla resistenza a frattura per trazione di fibre di carburo di silicio rivestite con matrice di titanio. Per rappresentare la variabilità della resistenza alla frattura di fibre di carburo di silicio della Amercom Trimarc, sono state utilizzate le statistiche di Weibull. Si è evidenziata una significativa variazione della resistenza in funzione della lunghezza di riferimento (1, 20 a 100 millimetri), dopo asportazione della lega di titanio con pulitura elettrolitica. E' stata condotta una prova mediante la tecnica di localizzazione lineare con due sensori acustici. La rottura si è verificata entro il tratto di riferimento ed eventi di 98 dB con ele-

vato rilascio di energia sono indicativi di rottura della fibra. La frattografia ha mostrato che le fibre con minore resistenza sono soggette a rottura a partire da difetti superficiali, mentre l'inizio di frattura a cuore è tipico delle fibre ad alta resistenza. Una funzione di Weibull cumulativa bi-modale, relativa alla probabilità di rottura, si è rivelata adeguata per caratterizzare i due diversi meccanismi di frattura all'interno della popolazione di fibre con lunghezze di riferimento di 1 e 20mm.

Le prove di fatica mostrano che la resistenza dei monofilamenti può peggiorare in caso di carico ciclico e il relativo meccanismo può essere identificato mediante la frattografia. I difetti della matrice, indotti dal processo, danno inizio alle cricche di fatica. Durante le prove di fatica, tensione-tensione, nel monofilamento si è verificato un distacco fra lo strato di carbonio ricoprente e la fibra di carburo di silicio.